

Chapter 6

STUDIES OF 1-AZACARBAZOLE IN BULK PROTIC SOLVENTS – II. WATER AND AMIDES

6.1 Introduction

Like the reactions in the diols, the observed rates attributed to reaction of 7AI and 1AC in water appear anomalously slow when plotted on the $E_T(30)$ polarity scale.^{1,2} This behavior for 7AI has been examined extensively without convergence to a clear understanding.³⁻²¹ Disagreement remains, for example, on the actual rate of tautomerization of 7AI in water. Petrich and coworkers suggest that only a small fraction of 7AI reacts quickly (~20% at ~70 ps, measured in emission and transient absorption experiments).⁶⁻¹⁸ On the other hand, Chapman and Maroncelli have argued that the tautomerization is slower (~830 ps in water) and that the nonradiative decay rate of the tautomer formed is much faster ($5 \times 10^9 \text{ s}^{-1}$) than in alcohols.⁵ For this reason, only one fluorescence band is observed for 7AI in water, as the tautomer emission is weak and is partially hidden under the normal band.^{5,3,19} Examination of the reaction of 1AC in water is therefore warranted to help to clarify the interpretation of the observed rates in both solutes.

The steady-state and time-resolved fluorescence spectroscopy of 1AC in water is reviewed first and is discussed within the context of the results of Chapter 5. Two

additional studies then explore the nature of the 1AC emission in water. An examination of the pH dependence of the 1AC reaction in water confirms that it is the neutral species present in the excited-state reaction. In the subsequent section, the dependence of the rates observed in mixed water-methanol systems indicates that a rapid solvent exchange model describes the observed kinetics and that the reaction of 1AC in water is indeed slow.

The chapter concludes with a discussion of the excited-state reaction of 1AC catalyzed by yet another family of bulk protic solvents: the amides. This work complements the study of the reaction of 1AC in isolated complexes involving amides and lactams presented in Chapter 4. The reaction rate of 1AC in bulk protic solvents is again observed to be significantly slower than in the isolated complexes.

6.2 Photochemistry of 1AC in Water

6.2.1 Steady-State and Time-Resolved Spectroscopy

At room temperature, the steady-state fluorescence spectrum of 1AC in water or deuterium oxide appears as a single broad band, unlike the dual fluorescence observed in the alcohols. As shown in *Figure 6.1*, deuteration of the solvent methanol slows the proton-transfer rate and leads to decreased intensity in the region of tautomer emission.

In water the reaction rate is believed to be even slower than that in methanol, and the tautomer emission in water correspondingly lacks distinction from the normal emission.

The time-resolved emission of 1AC in water is unlike that measured in the bulk alcohols: emission [excited at 290 or 306 nm] from ~20 nm spectral windows across the band may be fit with one lifetime, and no tautomer rise (deactivation) time is cleanly resolved by the time-correlated single-photon-counting spectrometer. (In the deuterium oxide temperature dependence study, a ~0.9 ns lifetime with small amplitude was observed in the tautomer region, but this emission is attributed to protonated 1AC.) At 25 °C, the observed (reaction) rates of 1AC in water and deuterium oxide are 2.32 ns and 7.35 ns, respectively, indicating an isotope effect (3.2) slightly smaller than for reactions in alcohols (~5) (see Chapter 7). The isotope effect of 1AC in water (3.2) is considerably greater than the isotope effects anticipated for the normal decay times (~1 since no proton or deuteron is transferred) or observed for the tautomer decay times (1.6 ± 0.2 ; see Chapter 7). This large isotope effect also supports the interpretation that the observed decay time of 1AC in water is most likely the reaction time.

The temperature dependence of the observed (reaction) rates are summarized in *Figure 6.2* and *Table 6.1*, and show that the isotope effect is independent of temperature and that the Arrhenius activation energy is ~60% of that for viscosity (*Table 5.11*).

6.2.2 Solvation Dynamics in Water

This apparently slow reaction in water is quite interesting. Various measurements indicate that “solvation dynamics” is very rapid in this solvent,^{22,23} although such

“solvation dynamics” may actually be introducing concepts that are inappropriate for understanding the problem at hand. In Chapter 5, the observed (reaction) rates for the diols and alcohols were compared with the solvent dielectric relaxation rates as a measure of cooperative hydrogen-bond dynamics. Like the alcohol and diol data presented there, the observed rates in water are also directly and linearly related to the rapid water relaxation times. As illustrated in *Figure 5.9*, the observed (reaction) rate for water normalized by the Debye relaxation rate lies along the linear correlation with primary alcohols and diols on the $E_T(30)$ solvent polarity scale. This suggests that the slow observed rate normalized by a measure of the hydrogen-bonding dynamics in water is consistent with the high polarity or hydrogen-bond strength of water measured on the $E_T(30)$ scale.

6.2.3 pH Dependence of 1AC in Water

The photochemical behavior of 1AC in water was surveyed for a wide pH range in order to determine the species fluorescing at neutral pH. In order to make stable measurements near pH=7, it was necessary to use a buffer (MES, 4-morpholine-ethanesulfonic acid, $pK_a = 6.1$). 1AC fluorescence lifetimes and steady-state emission band shapes showed little difference at neutral pH with or without added buffer.

Absorption and emission spectra from an acidic spectrophotometric titration are presented in *Figure 6.3* and *Figure 6.4*. The absorption spectra indicate a ground-state equilibrium ($pK_a = 4.0 \pm 0.1$) established between 1AC and 1AC-H⁺. The absorption of the protonated form 1AC-H⁺ is red-shifted with respect to the neutral form 1AC. The

emission spectra excited at the isobestic point (330 nm) also reveal the presence of at least two species with one isoemissive point at ~540 nm. At extremes in the pH range, emission from only one species is apparent: at high pH = 2, 1AC-H⁺ emits with $\lambda_{\max} \sim 480$ nm; and, at neutral pH = 6-8, 1AC emits with $\lambda_{\max} \sim 400$ nm. Plots of the total fluorescence intensities or normalized intensities at given wavelengths as a function of pH (*Figure 6.5*) all suggest that the excited-state emission reflects the underlying ground-state equilibrium ($\text{pK}_a \sim 4$).

Time-resolved emission decays recorded at different wavelengths and pHs support the identifications made in the steady-state spectra. For excitation at the isobestic point at 331 nm, the emission at 480 nm is characterized by one lifetime at high pH ($\tau = 0.98$ ns, 20 °C, pH <2.5), by one lifetime at neutral pH ($\tau = 2.5$ ns, 20 °C, pH 5-8), and by some combination of these two lifetimes at intermediate pH. (See *Table 6.2* for representative lifetimes.) Since the decays were fit well with constrained lifetimes, the following model of non-interconverting species is used to explore the connection between the normalized amplitudes and the populations of two species.

The time dependence of the fluorescence is given by

$$F(\lambda, t) = f_A(\lambda) k_{\text{rad}}(A) A^*(t) + f_{\text{AH}}(\lambda) k_{\text{rad}}(\text{AH}) \text{AH}^*(t) \quad (6.1)$$

where $A^*(t)$ and $\text{AH}^*(t)$ describe the time-dependence of the total normal 1AC and protonated 1AC-H⁺ populations, $f_X(\lambda)$ describes the fraction of species X emitting at the noted wavelength normalized such that $\int f_X(\lambda) d\lambda = 1$, and $k_{\text{rad}}(X)$ are the radiative rates determined at the appropriate acidic and neutral ends of the titration. The populations $A^*(t)$ and $\text{AH}^*(t)$ are described by single exponential decays $X^*(t) = X_o^* \exp(-t/\tau_X)$ as

noted earlier. Necessary data for the model are obtained from the steady-state spectra at appropriate pH levels: the quantum yield of protonated 1AC is $\sim 1/10$ that of the neutral species in water; $f_A(400\text{ nm}) = 1.15 \times 10^{-2}$, $f_{AH}(400\text{ nm}) = 3.62 \times 10^{-4}$, $f_A(480\text{ nm}) = 2.46 \times 10^{-3}$, and $f_{AH}(480\text{ nm}) = 7.53 \times 10^{-3}$.

The normalized amplitudes of the time-resolved emission

$$F(\lambda, t) = a_A \exp(-t/\tau_A) + a_{AH} \exp(-t/\tau_{AH}) \quad (6.2)$$

are identified with terms in Equation 6.1 and renormalized to yield the relative populations of 1AC and 1AC-H⁺. These values are summarized in *Table 6.2*.

The spectrophotometric titrations thus reveal ground-state equilibrium ($pK_a = 4.0 \pm 0.1$) and an equilibrium value in the excited-state that really reflects the ground-state equilibrium ($pK_a \sim 4$). Little change occurs in the populations in the excited-state because equilibrium is apparently not established during lifetime of the excited-state of 1AC in water. The Förster cycle may be used to estimate the pK_a^* corresponding to an excited-state equilibrium proton exchange.²⁴

The Förster cycle method is based on the thermodynamic equivalence of all routes leading from the ground-state acid (or base) to the thermally-equilibrated conjugate base (or acid) in the lowest excited singlet state. A Förster cycle is illustrated in *Figure 6.6*. In the ground and excited states, equilibria may be written between the species 1AC and 1AC-H⁺ and between 1AC* and 1AC-H⁺*, respectively. The electronic transition energies (E_{1AC} and E_{1AC-H^+}) between the ground and lowest excited states may be estimated from steady-state absorption or emission spectra. The entropies of protonation in the ground and excited states are assumed to be identical so that the enthalpies may be

expressed as free energies ΔG and ΔG^* . The change in energy between 1AC-H⁺ and 1AC* may then be expressed using two thermodynamically equivalent routes:

$$E_{1AC} + \Delta G^* = E_{1AC-H^+} + \Delta G, \text{ or} \quad (6.3)$$

$$\Delta pK_a = pK_a - pK_a^* = (E_{1AC} - E_{1AC-H^+}) / (2.303 R T) \quad (6.4)$$

$$pK_a - pK_a^* = [(N_A h) / (2.303 R T)] (\nu_{1AC} - \nu_{1AC-H^+}).$$

In the last expression, N_A is Avogadro's number, h is Planck's constant, R is the universal gas constant, T is the absolute temperature of the reaction, and ν is the frequency of radiation involved in the transition from the ground to lowest excited state.

Using the mean of the long-wavelength absorption and the short-wavelength emission to estimate the frequencies $\nu_{1AC} = 27780 \text{ cm}^{-1}$ and $\nu_{1AC-H^+} = 25000 \text{ cm}^{-1}$, we estimate the difference in equilibrium constants to be $pK_a - pK_a^* = 5.9$. The excited-state equilibrium constant is thus estimated to be $pK_a^* \sim -2$. This means that 1AC-H⁺ is a stronger acid (and 1AC a correspondingly weaker base) in the excited state, so that the concentration of 1AC in the excited state at neutral pH increases significantly compared to 1AC-H⁺. *Table 6.2* indicates an additional rapid quenching process occurs in strongly acidic solutions, but this effect vanishes by neutral pH levels where we wish to measure the rate of excited-state tautomerization in water.²⁵ Thus, 1AC is the only species observed by these time-resolved fluorescence measurements at neutral pH.

The pH dependence of 1AC has been reported in earlier studies. An early paper simply noted that "the acidity of the pyrrole proton and the basicity of the aza-nitrogen increase by 1.3 and 1.8 pK units respectively."²⁶ A later analysis applied the Förster cycle to steady-state absorption and emission spectra to calculate significant changes in

the equilibrium constants between the ground- and excited-states: for $1AC-H^+/1AC$, $pK_a = 4.2 \pm 0.2$ and $\Delta pK_a = +7.5 \pm 0.5$; for $1AC/1AC^-$, $pK_a = 14.3 \pm 1.0$ and $\Delta pK_a = -10.8 \pm 1.0$.^[27] The latter equilibrium constants indicate that $1AC^-$ is a stronger base (and $1AC$ a correspondingly weaker acid) in the excited state, so that the concentration of $1AC$ in the excited state at neutral pH again increases significantly compared to $1AC^-$.

The ground-state equilibrium constant for $1AC-H^+/1AC$ determined in this work is in good agreement with the previously reported value.²⁷ The observed ΔpK_a compared to the ΔpK_a predicted by the Förster cycle suggests that the proton-exchange equilibria between $1AC$ and $1AC-H^+$ and between $1AC$ and $1AC^-$ are not established in the excited state. Since the primary focus of this pH study was to determine the species emitting at neutral pH, careful investigations of the photochemical behavior of $1AC$ in regions of extreme pH (which often involve additional quenching mechanisms) were not pursued. We conclude that $1AC$ (as it reacts to form the tautomer) is the primary species observed at neutral pH.

The pH dependence of $7AI$ is very similar to that of $1AC$. The ground state equilibrium constants are $7AI-H^+/7AI$, $pK_a = 4.5 \pm 0.1$ and $7AI/7AI^-$, $pK_a = 12.1$.^[28,12,17] Like $1AC$, two sets of excited-state equilibrium constants have been proposed based on two different analysis methods. Förster cycle analysis predicts $\Delta pK_a = +8.3$ for the N_1-H proton in the excited-state.²⁹ Direct steady-state and time-resolved emission titrations, on the other hand, have indicated that the excited-state equilibrium constants change little

from the ground-state values.^{4,11,12,17} It appears that excited-state equilibrium may not be achieved for 7AI.

The charge redistribution in the excited-state that leads to shifts in acid and base strengths is implicated as the driving force for the proton-transfer reactions.³⁰ INDO/S calculations suggest that the driving force is smaller for 1AC than for 7AI,²⁷ which is certainly consistent with the observed rates attributed to the excited-state tautomerizations in water. The discrepancy between the Förster cycle analysis and the direct fluorescence measurements does suggest that equilibrium is not achieved during the fluorescence lifetime. The slow tautomerization rates deduced from the emission lifetimes are also consistent with a small driving force for these reactions in water.

6.3 Proton-Transfer Reactions in Methanol / Water Mixtures

6.3.1 1AC in Methanol/Water Mixtures

The absence of a rise (deactivation) time in the tautomer emission of 1AC in water is one distinguishing feature that could indicate that the reaction in water is different than in the alcohols and diols. Since few pure solvents are available with which to bridge the gap in polarity between water and methanol, a series of mixtures of methanol and water were used to explore the spectroscopy of 1AC in solvents of intermediate polarity.

The steady-state normal emission band red-shifts monotonically and the band width broadens almost linearly with increasing water concentration (*Table 6.3*).³¹ The time-resolved spectroscopy reveals that the normal emission may be fit with a single lifetime³² and that the tautomer emission may be fit with dominant rise and decay lifetimes, as summarized in *Table 6.3*. As the water concentration increases, the rate attributed to proton-transfer decreases monotonically, and the rate attributed to tautomer deactivation (1/rise time) increases monotonically. Indeed, the experiment is unable to cleanly resolve a rise time in the tautomer emission of 1AC in water.

Chapter 3 reviewed a two-state kinetic model with rapid solvent exchange. The measured rates for 1AC in the methanol-water mixture clearly fall in the limit of rapid solvent exchange for this model, as shown by the linear relationship in *Figure 6.7* and the single-exponential decays. The continuous change in the observed decay time from pure methanol to pure water is also an indication that reaction is occurring in water and that the observed decay time is the reaction time.

6.3.2 Other Proton-Transfer Reactions in Methanol/Water Mixtures

Earlier studies of mixtures of water and methanol have employed proton dissociation reactions of photoacids as probes of the structure of water.³³⁻³⁵ Naphthol-type photoacids (R-OH) exhibit dissociation rates that increase with increasing concentration of water, and cationic photoacids (RNH₃⁺) display dissociation rates that increase in the water-rich region with addition of organic solvent prior to sharply decreasing in the organic-rich region.³³⁻³⁵ The observed rate dependence for 1AC is

unlike these photoacids, suggesting that the observed reaction is not one controlled by a proton-transfer to solvent like the naphthol-type photoacids.

6.4 Photochemistry of 1AC in Bulk Amides

The excited-state proton-transfer reaction of 1AC has been studied extensively in the alcohols, diols, and water. These molecules serve as catalysts in promoting the reaction. In this section, the proton-transfer reaction of 1AC in bulk amides is characterized for the first time (to our knowledge). This family of solvents serves as noncatalytic agents in the reaction, themselves undergoing change as the normal form of 1AC is transformed into the tautomer form. The experiments described here complement the study of the reaction in isolated complexes of 1AC with amides or lactams reported in Chapter 4.

6.4.1 Steady-State and Time-Resolved Emission Spectroscopy

An excited-state reaction is observed for 1AC in the neat solvents formamide (FA) and N-methylformamide (NMF), but no reaction is observed in the aprotic solvent N,N-dimethylformamide (DMF). This study in the bulk amides permits the effects of extended solvent hydrogen-bonding on the proton-transfer reaction to be explored in a different family of protic solvents. Although the steady-state emission spectra of 1AC in FA and NMF do not display prominent tautomer emission like those in bulk alcohols (*Figure 2.3*), the emission quantum yields do reveal other nonradiative pathways for

depopulating the excited normal form of 1AC as recorded in *Table 2.3*. Time-resolved emission spectra at 560 nm (the tautomer region) confirm the presence of an excited-state reaction: the fluorescence decays consist of both a rise-time and a decay-time. Lifetime measurements of 1AC at room temperature are summarized in *Table 2.3*, and representative time-resolved emission decays of 1AC in formamide are presented in *Figure 6.8*. The behavior of 1AC in these bulk solvents appears similar to that in diols and water noted above. The decay-time (equal for both the normal and tautomer) is attributed to the proton-transfer reaction and the rise-time is identified with the deactivation of the tautomer. The radiative rates of the normal and tautomer species help to substantiate this interpretation (see *Table 2.3*). (Measurement of an isotope effect in FA-d₂ to confirm the proton-transfer character of the reaction has not yet been successful.) It is remarkable that the proton-transfer rate has significantly decreased in these neat hydrogen-bonded liquids compared to the ultrafast rate observed in complexes with lactams and several amides discussed in Chapter 4. Although an ultrafast rate has not been measured directly in 1AC complexes with alcohols because of weak association, a similar rate decrease occurs in bulk alcohols as well.

The temperature dependence of the reaction has been measured over the range 0-60 °C and is presented in *Figure 6.9* and *Table 6.4* with comparison to the temperature dependence of the viscosity. The decay lifetimes attributed to the reaction show the strongest dependence on temperature, and the following Arrhenius activation energies are determined: 12.8 kJ/mol for the observed rate of 1AC in FA compared to 19.5 kJ/mol for FA viscous flow; and 14.6 kJ/mol for 1AC in NMF compared to 14.2 kJ/mol for NMF

viscous flow.^{36,37} The Arrhenius activation energies of the tautomer rise-lifetimes are similar for both formamide (7.6 kJ/mol) and N-methylformamide (7.0 kJ/mol), suggesting related physical mechanisms leading to the tautomer deactivation. The similarity between E_{act} and E_{η} for these solvents is analogous to the behavior of 7AI and 1AC in primary alcohols, diols, and water as summarized in *Table 5.11*.

6.5 Prompt Emission and the Irreversible Proton-Transfer Model

Since the excited-state tautomerization of 1AC is measurably fast in isolated complexes with several lactams and amides, the bulk amides provide a system in which to explore the possibility of prompt reaction. The amides' structure H-N-C=O has an excellent geometry for forming 1:1 complexes with 1AC, and it is possible that such 1AC:amide molecular complexes are formed in the bulk amide solvents. These "isolated" complexes would react more quickly than 1AC in a solvent environment having an extended hydrogen-bonding network. In this section, a discussion of the extent of reaction is discussed for amide solvents as well as for a number of the slower alcohol and diol reactions.

In Section 3.3 a two-state kinetic model was described with which one may estimate the fraction of the 1AC population that undergoes prompt fluorescence. Using Equation 3.13, we estimate that the fraction of the population of 1AC undergoing prompt fluorescence while reacting in methanol, methanol-OD, ethylene glycol, formamide and N-methylformamide is on the order of 5-10% for all these protic solvents. No correction for N^* contamination was applied in this first estimate.

A more careful estimate of the prompt emission fraction using Equations 3.14, 3.15, 3.16 and 3.17 follows. For the determination of the constant $c(\lambda)$, $f_N(\lambda)$ is estimated from the steady-state emission spectra of 1AC in acetonitrile broadened by convolution with a Gaussian function and shifted to match the FWHM of the normal emission band of each protic solvent. The function $f_T(\lambda)$ is estimated by a log-normal fit to the tautomer emission in methanol obtained by subtracting $f_N(\lambda)$ from the measured line showing dual fluorescence. For this work, the ratio of radiative rates is assumed to be independent of solvent and has a mean value equal to 9 ± 1 (Table 2.3). These corrections for the contamination of tautomer emission by normal species further reduce the calculated fractions undergoing prompt fluorescence: NMF (2%), FA (2%), MeOH (4%), MeOD (8%), and EG (7%). Based on these values, we conclude that only a very small amount of 1AC is incorporated into a cyclically hydrogen-bonded complex that allows the reaction to occur promptly following the excitation of 1AC. Thus nearly the entire reaction of 1AC in these bulk protic solvents is observed in the time-resolved emission. This experimental result is consistent with recent computer simulations that also reveal the rarity of cyclical hydrogen-bonded complexes prepared for prompt reaction.³⁸

6.6 Conclusion

Earlier studies indicated that the excited-state proton-transfer reaction of 1AC occurs in diols and water but at a much slower rate than might be expected based on a reaction rate correlation on the $E_T(30)$ solvent scale. Here and in the previous chapter, it has been argued that the reaction of 1AC in these solvents is not functionally different

than the reaction in bulk alcohols. In this chapter the following experimental evidence has been cited to support the argument. **(1)** An examination of the pH dependence of the 1AC reaction in water confirms that it is the neutral species present in the excited-state reaction near pH = 7. **(2)** The dependence of rates observed in mixed water-methanol systems indicates that a rapid solvent exchange model describes the observed kinetics and that the reaction of 1AC in water is indeed slow. **(3)** The dependence of rates observed in mixed water-methanol systems also suggests that it is unlikely that an ion pair like the naphthol-type photoacids is produced by the reaction.

A number of interesting papers have been published since this experimental work on 1AC in water was concluded. Chou and coworkers have fully resolved the excited-state proton-transfer reaction of 3-cyano-7AI in water: the normal species decays in 900 ps and the tautomer species shows a 900 ps rise time and a 3.3 ns decay time.⁴⁷ The deactivation rate of the tautomer is significantly decreased compared to the reaction rate in this 7AI analogue, and this allows the full reaction to be observed by time-resolved fluorescence spectroscopy. Thus Chapman and Maroncelli's interpretation⁵ that the reaction rate is much slower than the tautomer deactivation rate for 7AI in water is affirmed. Castleman and coworkers have observed proton-transfer in hydrated gas-phase 7AI (with 2-4 water molecules), but complete tautomerization remains to be resolved.⁴⁶ This molecular-beam experiment and others^{44,45} provide additional insight into the molecular geometry required for excited-state double proton transfer. Finally, theoretical models are beginning to provide molecular-scale insight into the reaction of 7AI in water.³⁹⁻⁴³ For example, Fernandez-Ramos *et al.* argue that in solution two water

molecules participate in the reaction.⁴¹ Based on their level of theory, it cannot be established with certainty whether this tautomerization is concerted or stepwise and should be described by tunneling or classical transfer. The authors do suggest, however, that their best estimate is a stepwise reaction with one-proton tunneling as the rate-determining first step.⁴¹

The excited-state proton-transfer reaction of 1AC in the bulk amides formamide and N-methylformamide has been characterized in this chapter as well. In the future it is recommended that the isotope effect be measured in these solvents cleaned of impurities. The experimental data may also be compared to computer simulations of the reaction.

The study of the reaction of 1AC in bulk protic solvents is concluded with an examination of kinetic isotope effects. Does the reaction involve the concerted or stepwise motion of protons? Progress toward understanding the reaction mechanism is documented in the next chapter.

Table 6.1: Temperature Dependence of 1AC Lifetimes in Water and Deuterium Oxide

	T (K)	a ₁	a ₂	τ ₁ (ns)	τ ₂ (ns)
1AC / H ₂ O					
Normal (λ _{em} = 410 nm)	283	1.00		2.86	
	293	1.00		2.48	
	298 *	1.00		2.30	
	303 *	1.00		2.18	
	313	1.00		1.90	
	323	1.00		1.73	
	298	0.83	0.17	2.42	0.63
Tautomer (λ _{em} = 555 nm)	283	1.00		2.87	
	293	1.00		2.49	
	298	1.00		2.35	
	303 *	1.00		2.20	
	313	0.97	0.03	1.89	4.16
	323	1.00	0.00	1.74	12.00
	298	0.83	0.17	2.42	0.63
1AC / D ₂ O					
Normal (λ _{em} = 410 nm)	283 *	1.00		9.05	
	293	1.00		7.91	
	298	1.00		7.48	
	303	1.00		7.00	
	313	1.00		6.23	
	323	1.00		5.58	
	298	0.97	0.03	7.42	0.66
	313	0.97	0.03	6.22	0.30
	298	0.76	0.24	7.28	0.67
Tautomer (λ _{em} = 555 nm)	283	0.69	0.31	8.77	0.73
	293	0.92	0.08	7.89	0.82
	298 *	0.76	0.24	7.28	0.67
	303 *	0.95	0.05	6.98	0.68
	313	0.93	0.07	6.25	0.81
	323	1.00		5.56	

An asterisk indicates the reported values are an average of at least two measurements. Measurements for which biexponential lifetimes were observed may contain a small amount of protonated 1AC.

Table 6.2: pH Study of 1AC: Time-Resolved Emission

pH	Free Fits						Constrained Fits: τ_1 fixed at 0.977 ns			Relative Populations	
	a_1	a_2	a_3	τ_1 , ns	τ_2 , ns	τ_3 , ns	a_1	a_2	τ_2 fit, ns	[1AC-H ⁺]	[1AC]
400 nm											
1.79	0.44	0.55	0.10	0.018	0.94	3.56	0.65			1.00	0.00
2.02	0.48	0.27	0.25	0.009	0.91	1.89	0.37	0.26	1.97	0.99	0.01
2.50	0.07	0.28	0.66	0.112	1.10	2.49	0.24	0.70	2.44	0.98	0.02
2.82		0.11	0.89		0.69	2.38	0.14	0.86	2.43	0.95	0.05
3.09		0.07	0.93		0.63	2.45	0.10	0.90	2.49	0.93	0.07
3.36		0.06	0.94		0.25	2.46	0.07	0.94	2.50	0.90	0.10
3.62			1.00			2.47	0.05	0.95	2.52	0.86	0.14
3.91			1.00			2.50					
4.31			1.00			2.51					
4.67			1.00			2.52					
5.02			1.00			2.53					
5.48			1.00			2.53					
6.00			1.00			2.53					
480 nm											
1.79	1.00			0.98			1.00			1.00	0.00
2.02	1.00			0.99			1.00			1.00	0.00
2.50	0.94	0.06		0.96	2.03		0.96	0.04	2.33	0.97	0.03
2.82	0.91	0.09		0.96	2.25		0.93	0.07	2.51	0.95	0.05
3.09	0.84	0.16		0.94	2.25		0.88	0.12	2.53	0.91	0.09
3.36	0.77	0.23		0.95	2.38		0.80	0.20	2.51	0.84	0.16
3.62	0.67	0.33		0.94	2.43		0.70	0.30	2.53	0.76	0.24
3.91	0.51	0.49		0.89	2.43		0.56	0.44	2.56	0.63	0.37
4.31	0.28	0.72		0.80	2.45		0.34	0.66	2.55	0.40	0.60
4.67	0.12	0.88		0.70	2.47		0.16	0.85	2.53	0.20	0.80
5.02	0.06	0.94		0.66	2.49		0.09	0.92	2.53	0.11	0.89
5.48		1.00			2.51		0.04	0.96	2.55	0.06	0.94
6.00		1.00			2.52			1.00		0.00	1.00

MES buffer was added to the water in order to help stabilize the pH measurements.

Table 6.3: Steady-State Emission Band Characterization and Observed Rates for 1AC in Methanol-Water Mixtures

% MeOH (by volume)	X (MeOH)	ν (low_1/2Max) 1000 cm ⁻¹	$\langle \nu \rangle$ 1000 cm ⁻¹	Width = FWHM 1000 cm ⁻¹
100	1.00	23.82 ± 0.01	25.880 ± 0.001	4.12 ± 0.02
90	0.80	23.50 ± 0.03	25.674 ± 0.002	4.34 ± 0.05
70	0.51	22.99 ± 0.04	25.32 ± 0.04	4.67 ± 0.01
50	0.31	22.66 ± 0.06	25.04 ± 0.03	4.76 ± 0.05
30	0.16	22.00 ± 0.03	24.58 ± 0.04	5.15 ± 0.01
10	0.05	21.674 ± 0.001	24.23 ± 0.01	5.11 ± 0.02
0	0.00	21.459	24.035	5.15

% MeOH	Normal τ_1 , ns	Tautomer rise τ_1 , ns	Tautomer τ_2 , ns	$1+a_T/a_{PT}$	Prompt emission	k_{obs} 10 ⁹ s ⁻¹	k^1 10 ⁹ s ⁻¹
100	0.52	0.29	0.54	0.06	0.06	1.92	3.50
90	0.59	0.27	0.64	0.13	0.08	1.69	3.70
70	0.87	0.24	0.87	0.23	0.08	1.15	4.21
50	1.16	0.19	1.16	0.42	0.07	0.86	5.41
30	1.61	0.11	1.59	0.67	0.05	0.62	9.35
10	2.09	0.02	2.01	0.49	0.01	0.48	46.5
0	2.34		2.48	1.00	0.00	0.43	

Top Table: Steady-State Normal Emission Band Characterizations. The frequency at the low-frequency edge at the half-maximum, the average band frequency, and the band width are summarized as a function of solvent composition. The uncertainties indicate the size of the difference between the two independent measurements averaged for the reported value.

Bottom Table: Observed Rates. Values are an average of two independent measurements made on different days. A third long lifetime with small amplitude required for fits to the tautomer emission has been omitted from the table. The value of $1+a_T/a_{PT}$ reflects the relative sizes of the amplitudes for the tautomer rise (a_T) and decay (a_{PT}) times, and the fraction of “prompt fluorescence” is calculated as described in the text without correction for normal band contamination.

Table 6.4: Temperature Dependence of 1AC Lifetimes in Bulk Amide Solvents

1AC / Formamide	T (K)	a ₁	a ₂	a ₃	τ ₁ (ns)	τ ₂ (ns)	τ ₃ (ns)
Normal (λ _{em} =400nm)	278.2	1.00			2.63		
	288.2	1.00			2.18		
	298.2	1.00			1.82		
	308.2	1.00			1.52		
	323.2	1.00			1.24		
	338.2	1.00			0.98		
Tautomer (λ _{em} =560 nm)	278.2	-0.90	1.78	0.12	0.31	2.56	4.70
	288.2	-1.17	2.06	0.11	0.26	2.14	4.50
	298.2	-1.29	2.20	0.10	0.24	1.79	4.31
	308.2	-1.49	2.41	0.08	0.22	1.51	4.25
	323.2	-1.85	2.76	0.08	0.19	1.23	4.10
	338.2	-2.11	3.03	0.08	0.17	1.00	3.90
1AC / NMF	T (K)	a ₁	a ₂	a ₃	τ ₁ (ns)	τ ₂ (ns)	τ ₃ (ns)
Normal (λ _{em} =400nm)	274.2	1.00			7.10		
	283.2	1.00			5.70		
	293.2	1.00			4.81		
	298.2	1.00			4.42		
	303.2	1.00			3.99		
	313.7	1.00			3.22		
	323.2	1.00			2.74		
	333.2	1.00			2.25		
Tautomer (λ _{em} =560 nm)	274.2	1.61	-0.61		7.25	0.35	
	283.2	1.29	-0.75	0.46	5.40	0.38	7.95
	293.2	1.80	-1.03	0.22	4.59	0.35	9.38
	303.2	2.00	-1.10	0.10	4.03	0.30	10.30
	313.7	2.19	-1.37	0.18	3.19	0.28	7.91
	323.2	2.51	-1.69	0.19	2.68	0.26	7.54
	333.2	2.58	-1.77	0.19	2.22	0.25	7.17

Emission was collected over a 14 ns time range for 1AC in Formamide and over a 27 ns time range for 1AC in N-Methylformamide.

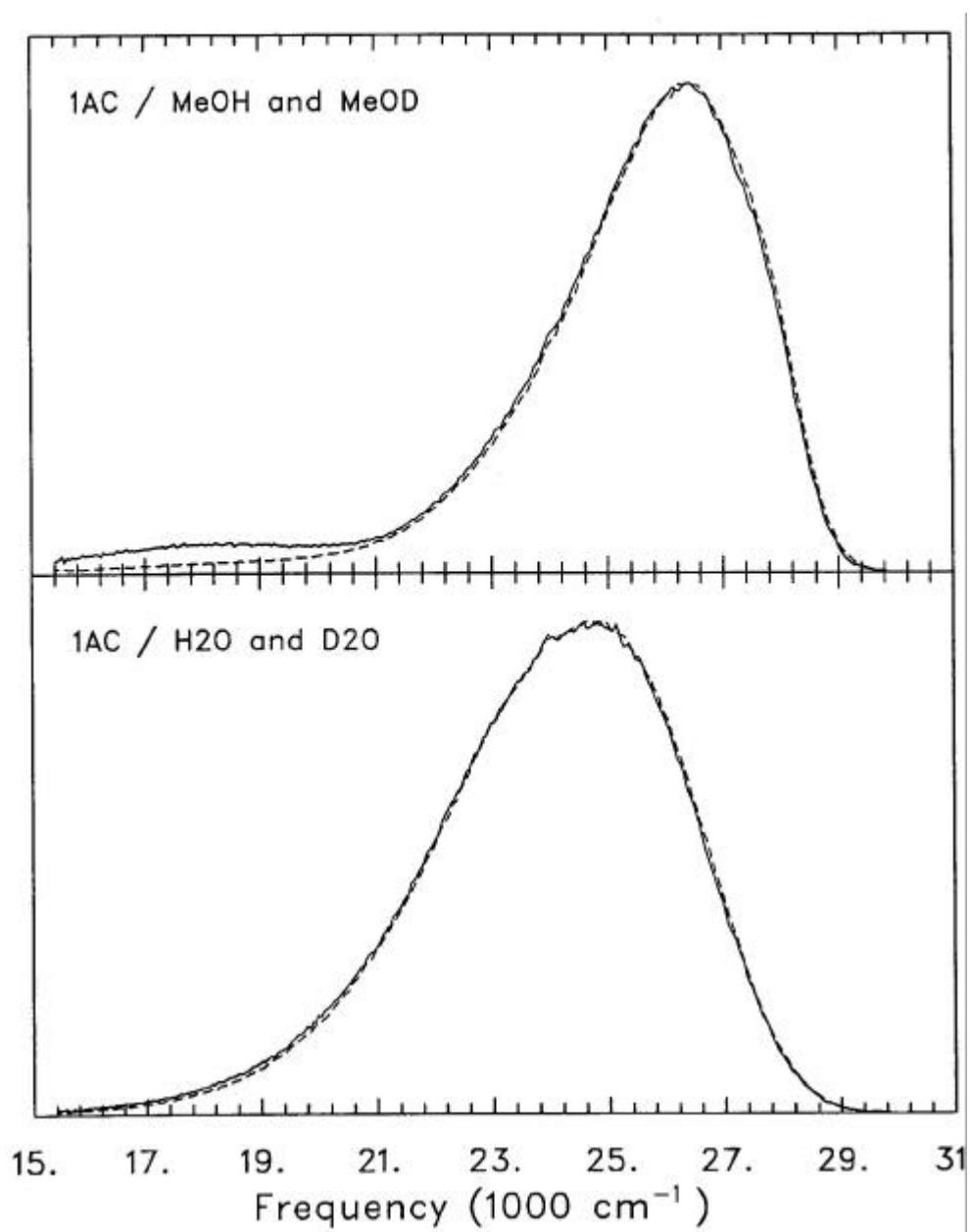


Figure 6.1: Comparison of Steady-State Emission Spectra of 1AC in Methanol or Methanol-OD and 1AC in Water or Deuterium Oxide

The (net) rate of tautomerization in water is much slower as revealed by the isotope effects on the emission spectra.

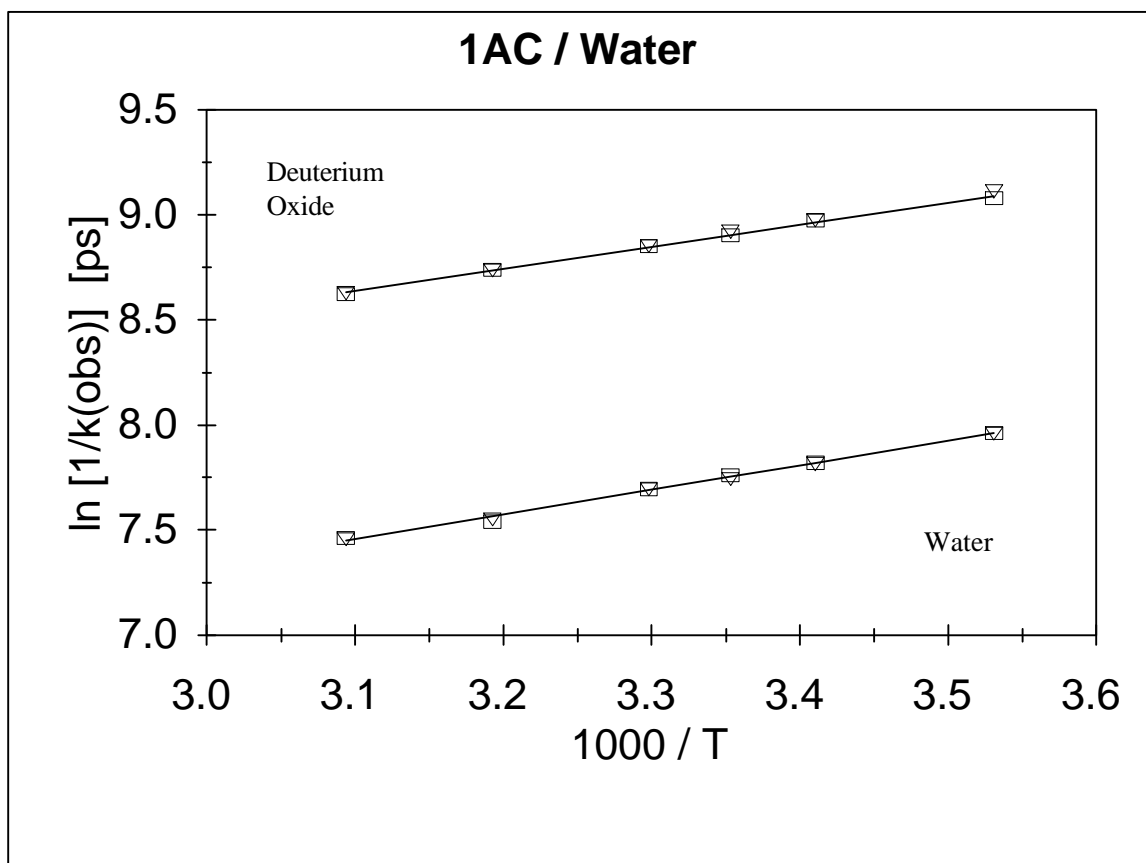


Figure 6.2: Temperature Dependence of 1AC Lifetimes in Water and Deuterium Oxide

Open triangles and squares represent normal (410 nm) and tautomer (555 nm) emission data, respectively.

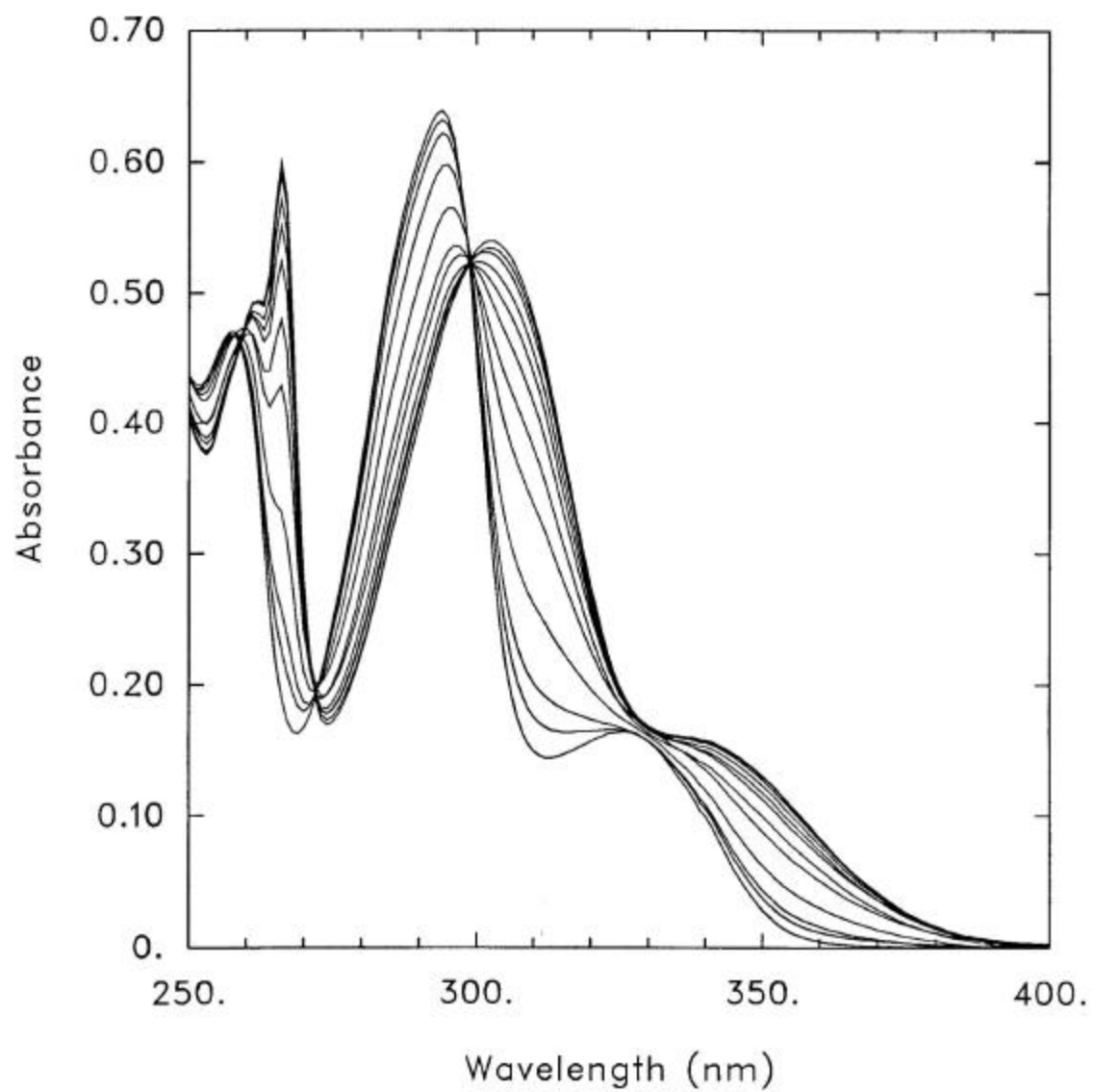


Figure 6.3: Spectrophotometric pH Titration of 1AC in Water with the Buffer MES

The absorption spectra red-shift with increasing acid concentration. The data cover the range pH = 2 – 6.

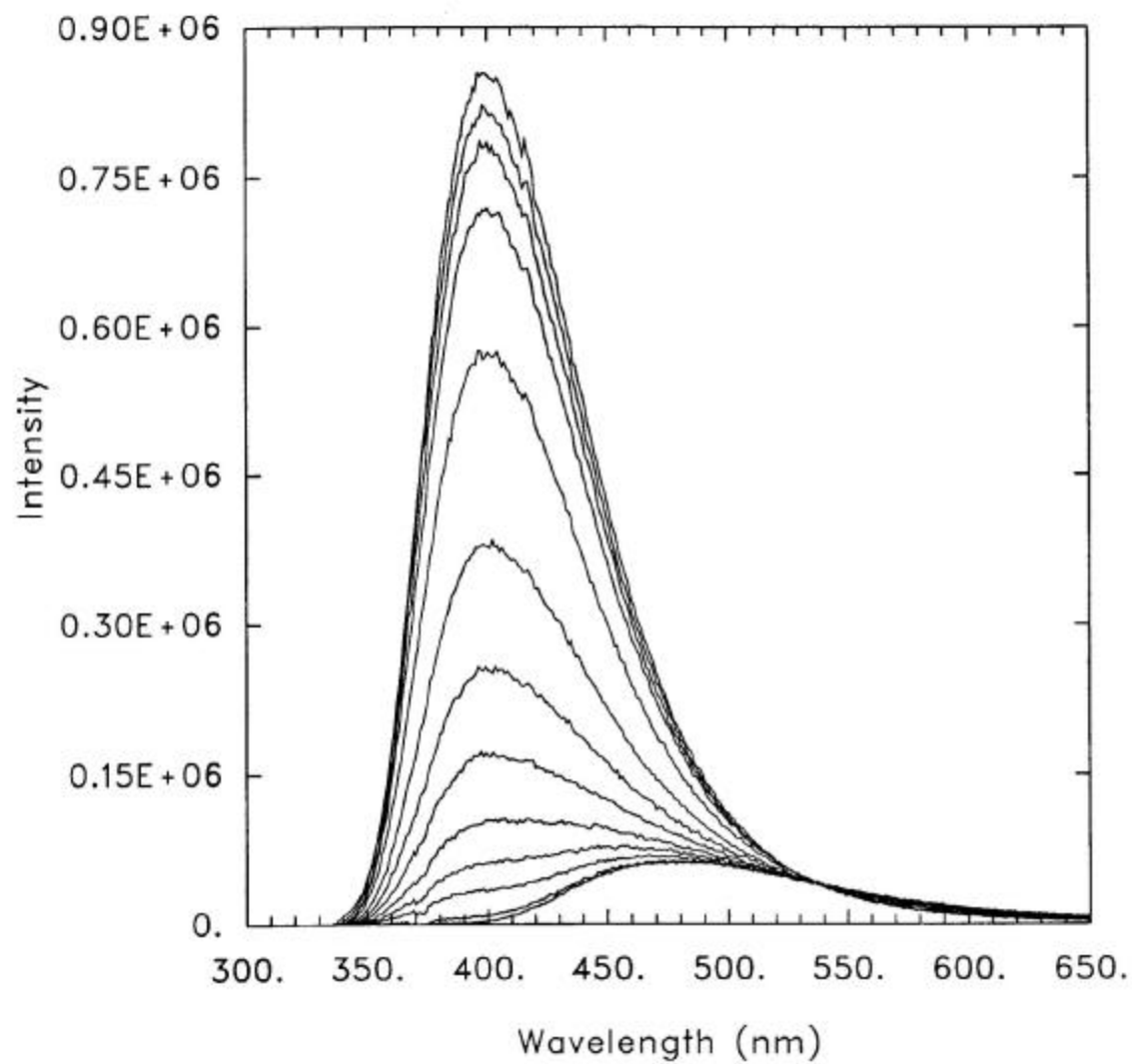


Figure 6.4: Spectrophotometric pH Titration of 1AC in Water with the Buffer MES

The emission spectra blue-shift with decreasing acid concentration. The data cover the range pH = 2 – 6.

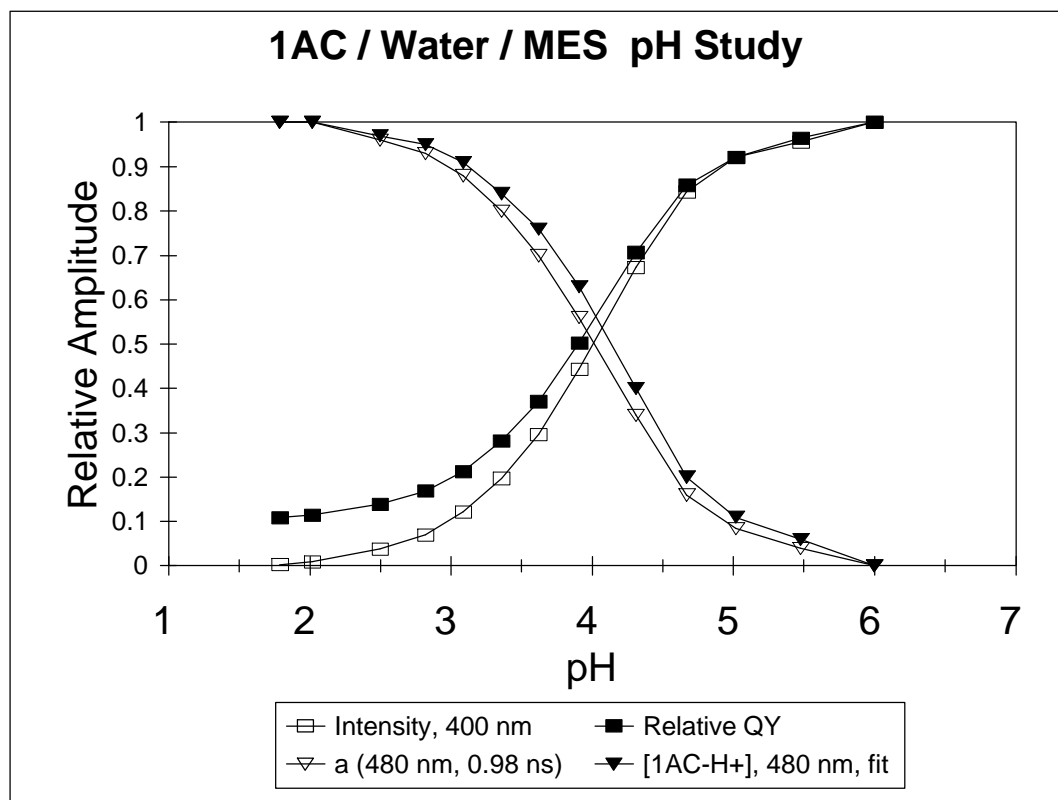


Figure 6.5: pH Study of 1AC

Plotted are three fluorescence measures for the spectrophotometric titration: relative emission intensity at 400 nm (open boxes), total relative quantum yield (solid boxes), and amplitude of the lifetime attributed to protonated 1AC (0.98 ns) (open triangles). The solid triangles represent the relative population of protonated 1AC. All emission characteristics point to $pK_a \sim 4$, the same as the ground-state.

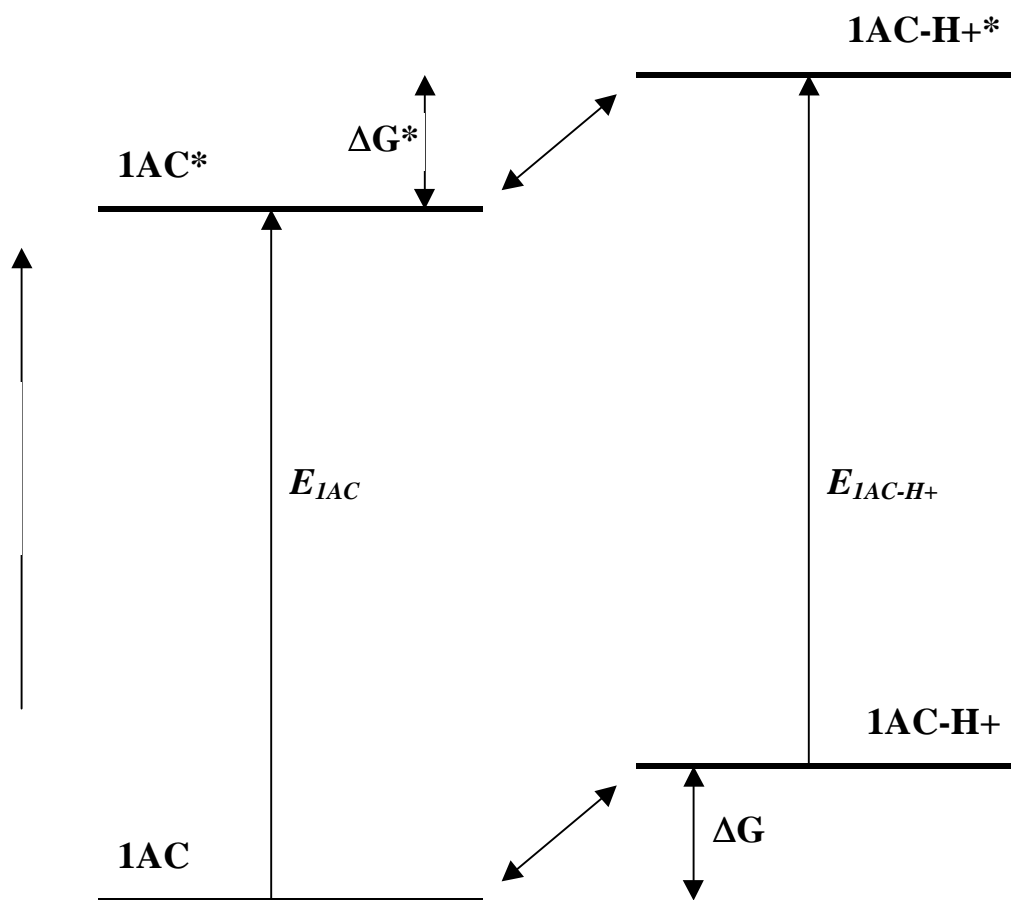


Figure 6.6: Schema of the Förster Cycle

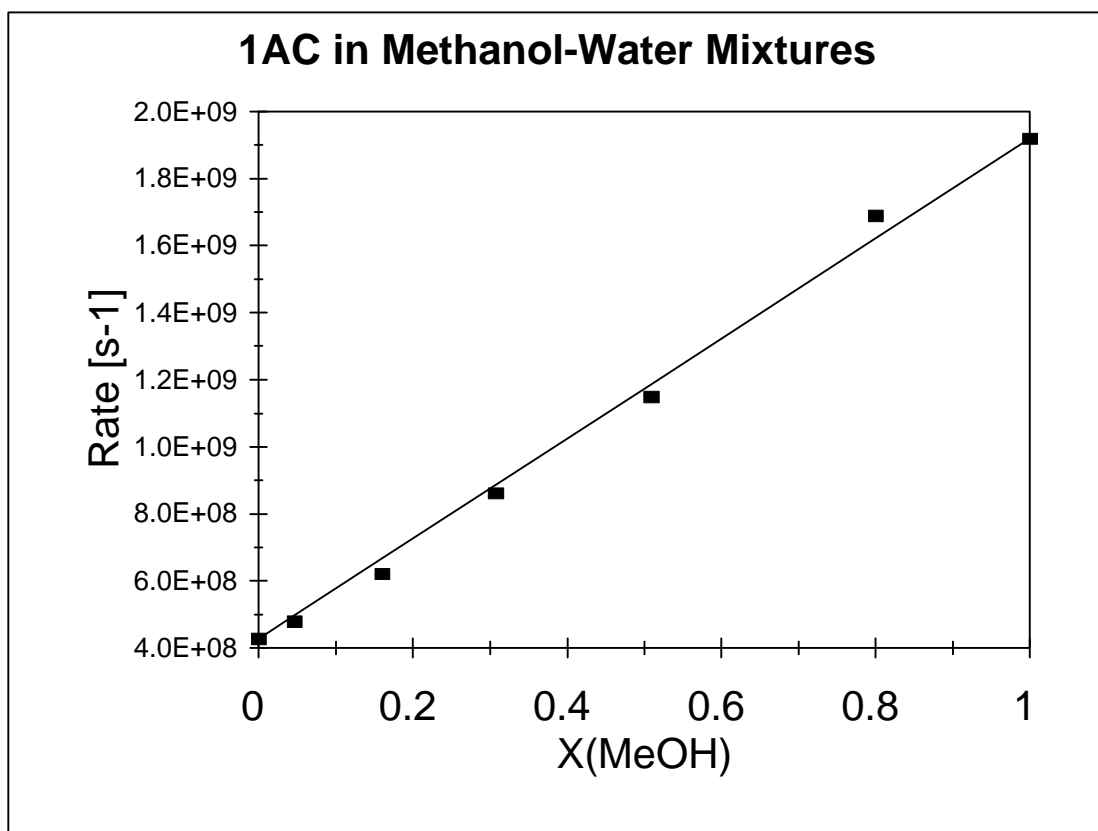


Figure 6.7: 1AC in Methanol-Water Mixtures: Time-Resolved Emission

The linear dependence of the observed on the composition of the solution indicates a rapid solvent exchange kinetic model is appropriate.

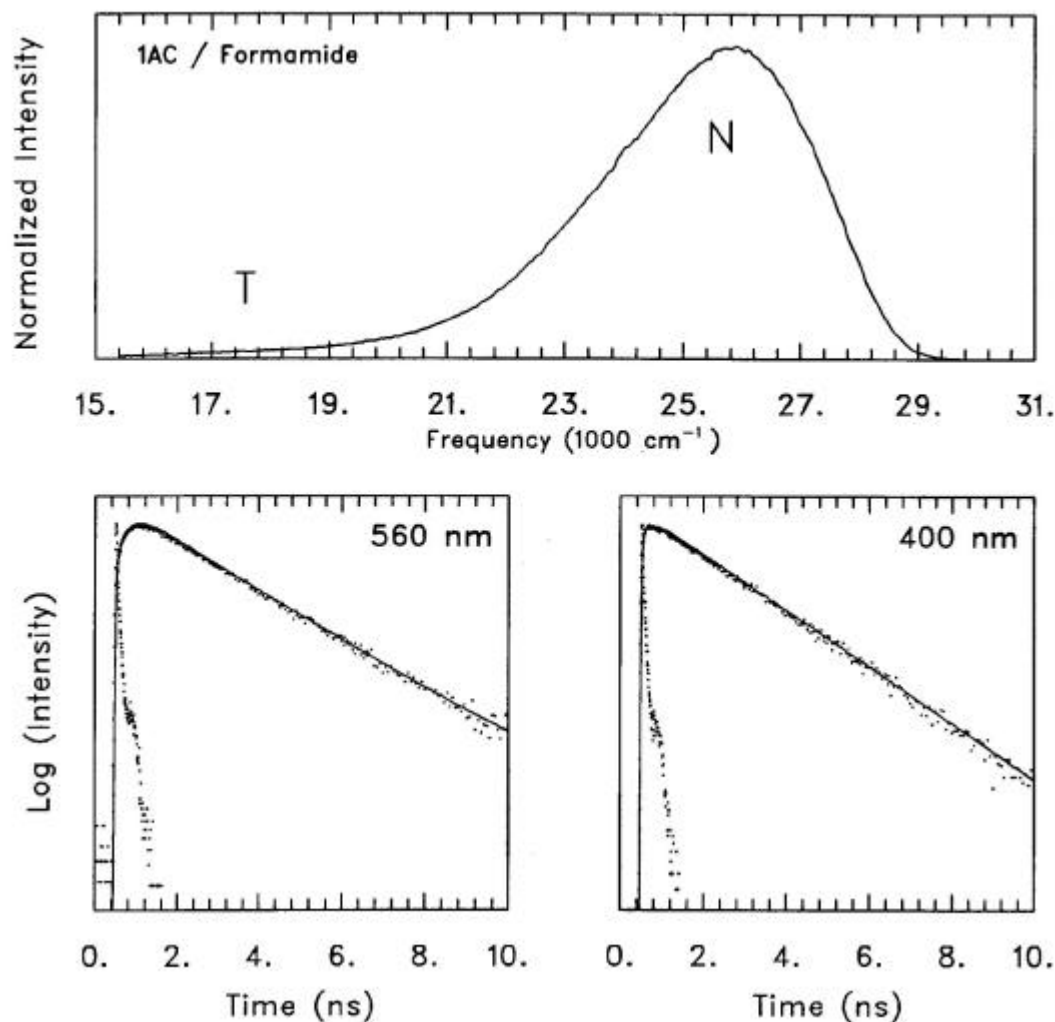


Figure 6.8: Fluorescence Spectroscopy of 1AC in Formamide at 293 K.

Top panel: Steady-state emission reveals predominantly the normal species emission. Bottom panels: Time-resolved emission decays were recorded in the normal (400 nm) and tautomer (560 nm) spectral regions:

$$N^*(t) / N(0) = (1.00) \cdot \exp(-t/1.92 \text{ ns}).$$

$$T^*(t) / T(0) = (-1.46) \cdot \exp(-t/265 \text{ ps}) + (2.28) \cdot \exp(-t/1.88 \text{ ns}) + (0.19) \cdot \exp(-t/3.4 \text{ ns})$$

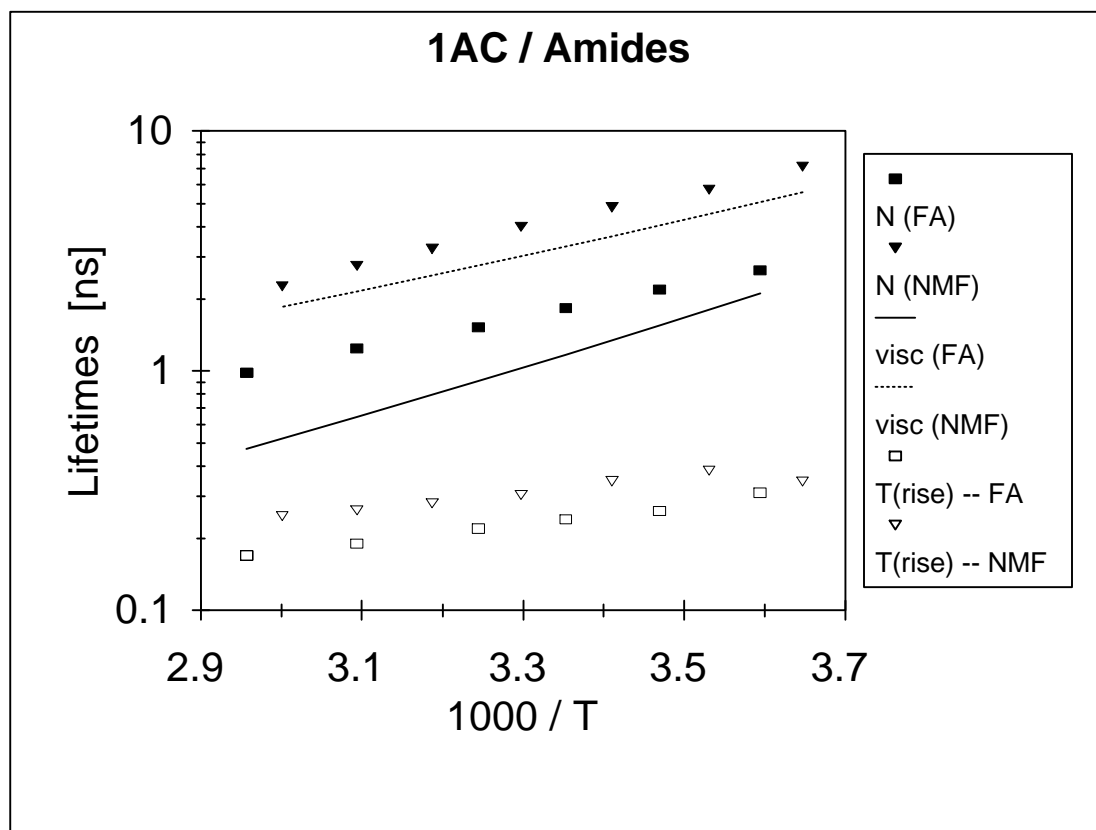


Figure 6.9: Temperature Dependence of 1AC Lifetimes in Formamide (FA) and N-Methylformamide (NMF).

Solid symbols are the normal lifetimes, and the open symbols are the tautomer rise-lifetimes. The temperature dependence of the viscosity (scaled) is plotted for comparison. [Viscosity data is from: (a) D. S. Viswanath and G. Natarajan, *Data Book on the Viscosity of Liquids*. (New York, Hemisphere Pub. Co., 1989). (b) C. L. Yaws, *Handbook of Viscosity*. (Houston, Gulf. Pub. Co., 1995).]

ENDNOTES

- ¹ R. S. Moog and M. Maroncelli, *J. Phys. Chem.*, **95**, 10359-10369 (1991).
- ² S. J. Boryschuk, M.S. Thesis, The Pennsylvania State University, 1993.
- ³ P. Avouris, L. L. Yang, and M. A. El-Bayoumi, *Photochem. Photobiol.*, **24**, 211 (1976).
- ⁴ K. C. Ingham and M. A. El-Bayoumi, *J. Am. Chem. Soc.*, **96**, 1674 (1974).
- ⁵ C. F. Chapman and M. Maroncelli, *J. Phys. Chem.*, **96**, 8430-8441 (1992).
- ⁶ A. V. Smirnov, D. S. English, R. L. Rich, J. Lane, L. Teyton, A. W. Schwabacher, S. Luo, R. W. Thornburg, and J. W. Petrich, *J. Phys. Chem. B.*, **101**, 2758 (1997).
- ⁷ R. L. Rich, F. Gai, Y. Chen, and J. W. Petrich, *SPIE*, **2137**, 435 (1994).
- ⁸ Y. Chen, F. Gai, and J. W. Petrich, *Chem. Phys. Lett.*, **222**, 329 (1994).
- ⁹ Y. Chen, F. Gai, and J. W. Petrich, *J. Phys. Chem.*, **98**, 2203 (1994).
- ¹⁰ F. Gai, R. L. Rich, and J. W. Petrich, *J. Am. Chem. Soc.*, **116**, 735 (1994).
- ¹¹ Y. Chen, F. Gai, and J. W. Petrich, *J. Am. Chem. Soc.*, **115**, 10158 (1993).
- ¹² Y. Chen, R. L. Rich, F. Gai, and J. W. Petrich, *J. Phys. Chem.*, **97**, 1770 (1993).
- ¹³ M. Negrerie, F. Gai, J.-C. Lambry, J.-L. Martin, and J. W. Petrich, *Ultrafast Phenomena VIII* (Springer Series in Chemical Physics, Vol. 55), (J.-L. Martin, A. Mingus, G. A. Mourou, and A. H. Zewail, eds.) (Berlin: Springer-Verlag, 1993). pp. 621-623.
- ¹⁴ M. Negrerie, F. Gai, J.-C. Lambry, J.-L. Martin, and J. W. Petrich, *J. Phys. Chem.*, **97**, 5046 (1993).
- ¹⁵ R. L. Rich, Y. Chen, D. Neven, M. Negrerie, F. Gai, and J. W. Petrich, *J. Phys. Chem.*, **97**, 1781 (1993).
- ¹⁶ F. Gai, Y. Chen, and J. W. Petrich, *J. Am. Chem. Soc.*, **114**, 8343 (1992).
- ¹⁷ M. Negrerie, F. Gai, M. Bellefeuille, and J. W. Petrich, *J. Phys. Chem.*, **95**, 8663 (1991).

- ¹⁸ M. Negreterie, S. M. Bellefeuille, S. Whitham, J. W. Petrich, and R. W. Thornburg, *J. Am. Chem. Soc.*, **112**, 7419 (1990).
- ¹⁹ P.-T. Chou, M. L. Martinez, W. C. Cooper, D. McMorro, S. T. Collins, and M. Kasha, *J. Phys. Chem.*, **96**, 5203 (1992).
- ²⁰ S. T. Collins, *J. Phys. Chem.*, **87**, 3202 (1983).
- ²¹ K. S. Pandey and P. C. Mishra, *Indian J. Pure & Applied Phys.*, **31**, 727 (1993).
- ²² See, for example, R. Jiminez, G. R. Fleming, P. V. Kumar, and M. Maroncelli, *Nature*, **369**, 471 (1994).
- ²³ C. Rønne, L. Thrane, P. Åstrand, A. Wallqvist, K. V. Mikkelsen, and S. R. Keiding, *J. Chem. Phys.*, **107**, 5319, (1997).
- ²⁴ S. G. Schulman, "Acid-Base Chemistry of Excited Singlet States: Fundamentals and Analytical Applications" in E. L. Wehry, editor, *Modern Fluorescence Spectroscopy, Volume 2* (New York, Plenum Press, 1976). Pp. 239-275.
- ²⁵ For other examples of proton-induced quenching, see H. Shizuka, *Acc. Chem. Res.*, **18**, 141 (1985).
- ²⁶ C. Chang, N. Shabestary, and M. A. El-Bayoumi, *Chem. Phys. Lett.*, **75**, 107 (1980).
- ²⁷ J. Waluk, A. Grabowska, B. Pakula, and J. Sepiol, *J. Phys. Chem.*, **88**, 1160 (1984).
- ²⁸ T. K. Adler and A. Albert, *J. Chem. Soc.*, 1794 (1960).
- ²⁹ H. Bulska, A. Grabowska, B. Pakula, J. Sepiol, J. Waluk, and U. P. Wild, *J. Lumin.*, **29**, 65 (1984).
- ³⁰ J. F. Ireland and P. A. H. Wyatt, *Adv. Phys. Org. Chem.*, **12**, 131 (1976).
- ³¹ Monte Carlo simulations of methanol-water mixtures by L. C. G. Freitas, *J. Mol. Struct.*, **282**, 151 (1993) indicate an enhancement of the number of hydrogen-bonded complexes at the methanol concentration $X=0.25$ which coincides with the maximum deviation from ideality for the mixture. The strongest deviations in the average emission frequency and its red-shift for 1AC also occur near this composition.

- ³² In some of the decays, a small amplitude (~10%) rapid lifetime (<150 ps) could be extracted from a fit to the normal emission. Since this component is not convincingly real, it is omitted from the discussion. If an average lifetime were calculated for the normal decay, this small component would have little effect.
- ³³ See, for example: E. Pines and G. R. Fleming, *J. Phys. Chem.*, **95**, 10448 (1991).
- ³⁴ A second example is discussed by N. Agmon, D. Huppert, A. Masad, and E. Pines, *J. Phys. Chem.*, **95**, 10407 (1991).
- ³⁵ A third example is discussed by G. W. Robinson, P. J. Thistlethwaite, and J. Lee, *J. Phys. Chem.*, **90**, 4224 (1986).
- ³⁶ C. L. Yaws, *Handbook of Viscosity*. (Houston, Gulf Pub. Co., 1995).
- ³⁷ D. S. Viswanath and G. Natarajan, *Data Book on the Viscosity of Liquids*. (New York, Hemisphere Pub. Corp., 1989).
- ³⁸ S. Mente and M. Maroncelli, *J. Phys. Chem. A*, **102**, 3860-3876 (1998).
- ³⁹ G. M. Chaban and M. S. Gordon, *J. Phys. Chem. A*, **103**, 185-189 (1999).
- ⁴⁰ M. K. Shukla and P. C. Mishra, *Chem. Phys.*, **230**, 187-200 (1998).
- ⁴¹ A. Fernandez-Ramos, Z. Smedarchina, W. Siebrand, and M. Z. Zgierski, *J. Chem. Phys.*, **114**, 7518-7526 (2001).
- ⁴² Z. Smedarchina, W. Siebrand, A. Fernandez-Ramos, L. Gorb, and J. Leszczynski, *J. Chem. Phys.*, **112**, 566-573 (2000).
- ⁴³ A. Fernandez-Ramos, Z. Smedarchina, W. Siebrand, M. Z. Zgierski, and M. A. Rios, *J. Am. Chem. Soc.*, **121**, 6280-6289 (1999).
- ⁴⁴ A. Nakajima, Y. Negishi, R. Hasumi, K. Kaya, *Eur. Phys. J.*, **D 9**, 303-307 (1999).
- ⁴⁵ H. Yokoyama, H. Watanabe, T. Omi, S. Ishiuchi, and M. Fujii, *J. Phys. Chem. A*, **105**, 9366-9374 (2001).
- ⁴⁶ D. E. Folmer, E. S. Wisniewski, J. R. Stairs, and A. W. Castleman Jr., *J. Phys. Chem. A*, **104**, 10545-10549 (2000).

⁴⁷ P.-T. Chou, W.-S. Yu, C.-Y. Wei, Y.-M. Cheng, and C.-Y. Yang, *J. Am. Chem. Soc.*, **123**, 3599-3600 (2001).